

Stanley S. Ipson, et. al.. "Vision and Image Sensors."

Copyright 2000 CRC Press LLC. <<http://www.engnetbase.com>>.

Vision and Image Sensors

Stanley S. Ipson
University of Bradford

Chima Okereke
University of Bradford

64.1 Image Formation

64.2 Image Sensing

Television Camera Tubes • Charge-Coupled Devices • Linear Charge-Coupled Devices • Area Charge-Coupled Devices • Photodiode Arrays • Serially Switched Photodiode Arrays • Charge-Coupled Photodiode Arrays

64.3 Image Intensifiers

Generation I Tubes • Generation II and III Tubes

64.4 Fiber-Optic Scopes

64.5 Components and Trends References

Vision is the act of seeing, a human capability derived from the combination of the image forming optical system of the eye, the array of light sensitive receptors in the retina of the eye, and the information processing capacity of the retina and human brain. Applications for instruments with a similar ability to sense a scene include broadcast television, monitoring industrial processes, quality control during manufacture, viewing inaccessible or hazardous places, aiding medical diagnosis, and remote sensing from satellites and space probes, to name but a few. Each application often has particular requirements more critical than others, and the problem is to find the most economical solution satisfying these most closely.

The human eye is a familiar imaging system, highly optimized to aid survival under the naturally occurring range of illumination conditions. It is useful to describe its basic characteristics [1] to provide a benchmark against which machine vision can be compared. Light intensity can be measured using radiometric quantities such as radiant power, which is the radiant energy transferred per second in watts; irradiance, which is the radiant power falling onto a surface of unit area in W/m^2 ; and radiance, which is the radiant power leaving unit area of a surface per unit solid angle in $W/st/m^2$. It can also be measured using photometric units that take into account the variation in response of a standard human eye with wavelength, the CIE (Commission Internationale de l'Éclairage) response curve. The photometric equivalent of radiant power is luminous flux, measured in lumens (lm); the photometric equivalent of irradiance is illuminance, measured in lm/m^2 or lux; and the photometric equivalent of radiance is luminance measured in $lm/st/m^2$ or cd/m^2 . At the wavelength of peak sensitivity (555 nm) in the CIE sensitivity curve, the conversion factor from radiometric to photometric units is 680 lm/W.

The eye has a response (observed brightness) to incident light intensity which is roughly logarithmic and is capable of adapting, given time, to an enormous range of different illuminance levels, from full sunlight (100,000 lux) to starlight (0.001 lux). The illumination generally recommended for surfaces in an office environment (about 100 lux) represents a comfortable working level. It takes about 30 min for

the eye to become fully dark adapted and a further 3 min to adapt again to increased lighting levels. Despite this adaptation capability, when viewing any one point in a scene under bright light conditions, the eye is capable of discerning only about 25 different intensity levels. The eye achieves its enormous range of brightness adaptation partly through the action of a variable size iris (about 2 to 8 mm in diameter), but mainly through the presence of two types of light sensitive receptor in the retina of the eye.

At high illumination levels, corresponding to photopic vision, the eye perceives color due to the excitation of three different types of cone receptors. There is considerable overlap in the spectral sensitivity curves of these red, green, and blue receptors, which have peak responses near 600, 550, and 500 nm, respectively. The overall photopic response is greatest at a wavelength near 555 nm in the yellow green region of the spectrum and falls to zero toward the red and the blue ends of the spectrum at about 750 and 380 nm, respectively. At low levels of illumination, corresponding to scotopic vision, only the rod receptors are excited with a peak luminous efficiency of about 1700 lm/W near 510 nm in the green region of the spectrum. The sensitivity to contrast of the dark-adapted eye is much poorer than that of the light-adapted eye. The transition between photopic and scotopic vision is gradual, with both excited over a luminance range from about 0.001 to 0.1 cd/m². The photopic response extends higher to the glare limit, about five orders of magnitude brighter, while the scotopic response extends lower to the threshold of vision, about three orders of magnitude lower. The photopic (CIE) and scotopic spectral responses of the eye are shown in Figure 64.1 with the response of a typical silicon-based sensor for comparison. The latter has a spectral response that is quite different from that of the human eye, extending well beyond the red end of the visible spectrum toward 1100 nm, with maximum sensitivity around 800 nm. Assuming the average spectral response of silicon, an irradiation of 1 μW/cm² corresponds to an illumination of about 0.22 lux.

The distribution of the cones and rods over the inner surface of the eyeball is nonuniform, with the cones most densely packed in the region of the fovea, a circular region about 1.5 mm in diameter situated toward the rear of the eyeball. To achieve sharpest vision, the eye muscles automatically rotate the eyeball so that the object of interest in the scene is imaged onto the fovea. The separation of the approximately 400,000 cones in the fovea is such that a normal young eye is able to distinguish alternating black and white bands, each 1 mm wide at a distance of about 5 m, corresponding to an angular resolution of about 0.2 mrad. The resolution of the dark-adapted eye is very much poorer because, although the maximum number of rods per square millimeter is similar to that of cones, several rods are connected to a single nerve end, whereas only a single cone is connected to a nerve end.

The overall performance of the eye is difficult to equal. However, a machine vision system can surpass it in individual respects such as sensitivity to infrared and ultraviolet radiations invisible to the eye, speed of response (which can be as short as nanoseconds), and sensitivity to low light levels corresponding to the detection of individual photons of radiation over periods of several hours. Machine vision charac-

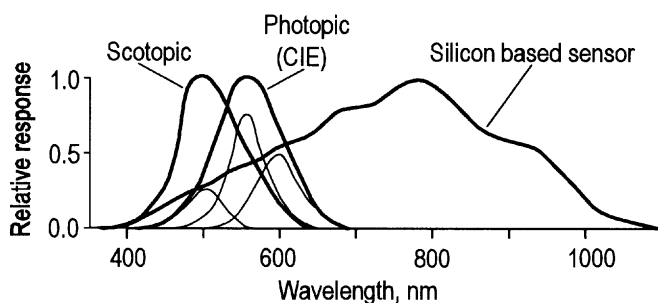


FIGURE 64.1 The linear responses, normalized to unity, of a typical bright-adapted human eye (photopic), a typical dark-adapted eye (scotopic) and a typical charge-coupled-device sensor to different wavelengths of light. The CIE response curve is an internationally agreed response curve for the photopic vision of a standard observer which is used to convert radiometric measurements to photometric. The individual responses of the red, green, and blue cones are also shown, drawn using thinner lines, beneath the photopic curve.

teristics depend on the type of image sensor employed and the modifying effects of additional components such as image intensifiers or optical fiber scopes. The machine vision equivalent of the eye includes a lens to project a 2-D image of the 3-D object of interest onto a sensor that transforms the light energy into an electrical signal. In this form, it may then be transmitted to a remote location, subjected to computer analysis, or displayed on a television screen. A rectangular 2-D image can be sensed using three different approaches. A single, small sensor can be moved in a zig-zag or raster fashion to sense the light intensity on a grid of points covering the whole image. A second approach is to use a line sensor composed of many individual sensors. If it is equal in length to one side of the image, it need only be moved in steps equal to the width of the individual sensors, a distance equal to the other side to cover the whole image. The third approach is to use an area sensor comprising a 2-D array of individual sensors. Whatever method is used, each individually sensed small region of the image is called a *picture element* or *pixel* and, in general, the resolution of the imaging system improves with increasing number of pixels. Although the first two methods require relative movement between sensor and scene, they are not limited by the sensor in the amount of resolution that can be achieved along the direction of motion. In addition, the inevitable variation in response between different sensors is easier to correct than with comparable area sensors, because there are fewer sensors. Two common applications of line sensors are monitoring objects on moving conveyer belts and scanning documents. In many cases, however, it is not practical to arrange relative movement of image and sensor, and the majority of image sensors in use are monochrome or color area sensors designed for use in television cameras. Monochrome and color cameras both use the same basic sensors, which have an inherently broad spectral response. Color sensitivity is achieved with the aid of color filters. A common approach is to deposit color filters directly on the sensor surface in a mosaic or stripe pattern. This is a cheap and compact solution but results in a lower spatial resolution in each color, compared with the resolution of the equivalent unfiltered sensor, and loses much of the incident light through absorption in the filters. Better sensitivity and resolution are obtained using three-sensor cameras that incorporate an optical arrangement (based on dichroic mirrors) that separates the incident light into three components—say red, green, and blue—which are each directed at a different sensor. However, this approach is both bulky and expensive, because it requires three sensors rather than one, and precision optics to align the images correctly on the individual sensors.

Most area sensors currently sold are designed to produce electrical signals compatible with either the 525-line American television standards (RS-170 for monochrome and NTSC for color) or the 625-line European television standards (CCIR for monochrome and PAL for color) [2]. These are interlaced television standards in which each complete image or frame is made up of two fields, each containing either odd or even numbered lines from the frame. Half the remaining lines, making up the odd total number in the frame, appear in each field, ensuring that the two fields interlace properly on the television display. Interlacing is used to avoid picture flicker without having to double the rate of information transmitted. According to the Ferry-Porter law, the critical frequency below which flicker is observed depends on the logarithm of the luminance of the picture highlights. At the brightness levels corresponding to normal viewing, flicker would be observable in pictures interrupted at 25 Hz or 30 Hz, but it is reduced to an acceptable level at the repetition rates of the fields (60 Hz for NTSC and 50 Hz for PAL). A consequence of the Ferry-Porter law is that an NTSC picture can be about six times brighter than a PAL picture and still be acceptable in terms of flicker. Many companies supply frame grabber computer boards that sample the TV-compatible voltage signals (about 1 V range) at a frequency of at least 10 MHz (for at least 512 samples per line), quantize the analog voltage to 256 or more discrete levels (8 bits), and store the resulting digital data for computer analysis. Interlaced operation is not ideal for some applications and, at higher cost, cameras are available that provide higher frames rates, higher resolutions, or progressive scan (no interlacing). These usually produce a standard digital output signal for easy input into a computer. A very wide range of sensors and cameras are currently commercially available, based on several different types of technology. Although each technology has particular advantages, the characteristics of different devices based on a specific technology can vary significantly. For example, the spectral responses of photodiode-based sensors generally extend to shorter wavelengths than those of CCD (charge-coupled device)-based sensors, but some CCD devices are available with extended blue-

end responses. Improved and/or cheaper sensors and cameras are appearing on the market all the time and, when considering a new imaging system, it is wise to review the characteristics of the devices currently available in comparison with the requirements of the application in order to select the most suitable. One of the first steps in the creation of a machine vision system for a new application is the design or selection of an appropriate optical system, and this is the subject of the next section. Later sections discuss the various sensor technologies that are available and other related devices that can be used to improve sensitivity or to allow image sensing in restricted spaces such as body or machine cavities.

64.1 Image Formation

The machine vision optical system has the tasks of matching the required field of view to the dimensions of the sensor and gathering sufficient light to achieve a sensor signal that has adequate signal-to-noise ratio (SNR) while maintaining the image sharpness required by the application. Resolutions of area sensors are sometimes specified by manufacturers as the maximum number of horizontal TV lines that can be distinguished. This value may be obtained from measurements of the visibility of a test chart (EIA test pattern), or it may simply be the number of horizontal pixels divided by 1.33, in the case of a monochrome sensor. In special circumstances, measurements to subpixel accuracy can be achieved by interpolation between pixel values, and Reference 3 describes the measurement of a knife edge to about 0.1 pixel accuracy. As a rule of thumb, however, for size measurement applications, the sensor should have a number of pixels at least equal to twice the ratio of the largest to smallest object sizes of interest [4], and a lens is then selected to provide the required magnification and working distance. A lens operating in a single medium such as air is characterized [5] by two focal points and two principal planes as indicated in Figure 64.2. The principal planes coincide with the lens center in the case of an ideal thin lens but may be separated by +20 to -10 mm (the negative sign indicating reversed order), depending on the design, in multielement lenses. They can be determined by first locating the two focal points and then measuring along the axis from these, distances equal to the focal length. A lens of focal length f produces an image in best focus at a distance l_i when the object is at distance l_o where

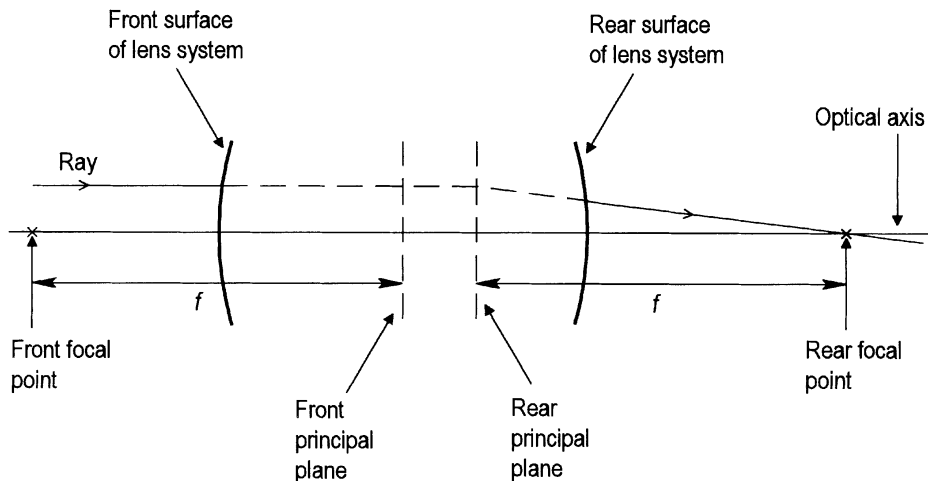


FIGURE 64.2 The trace of a ray from a distant object through a typical multielement lens system showing typical positions of focal points and principal planes. The distance from the back focal length to the lens flange mount is 17.3 mm for C-mount lenses, 12.5 mm for CS-mount lenses, and 46.5 mm for 35 mm photographic format Nikon F (bayonet) mount lenses. Adapters are available to accommodate the differences in distances and fittings of the different mounting systems.

$$\frac{1}{l_o} + \frac{1}{l_i} = \frac{1}{f} \quad (64.1)$$

and the distances are measured to the corresponding principal planes. The image magnification m , defined as the ratio of image to object size, is equal to the ratio of the image to object distances and is related to the total distance between object and image D_T by

$$D_T = \frac{F(m+1)^2}{m} + D_N \quad (64.2)$$

where D_N is the separation between the principal planes. Lenses generally have a focusing adjustment of 5 to 10% of the focal length, and extension rings between the lens and sensor are required for image magnifications greater than about 0.05. The lens extension required is simply the product of the magnification and the focal length. The depth of field F_o of an imaging system [6] is the displacement of the object along the optic axis that produces no significant degradation in the sharpness of the image. The corresponding movement of the image is the depth of focus. In the case of a lens with f /number $f_\#$ (equal to the ratio of focal length to lens iris diameter) and an image sensor with pixel size P , it is given by

$$F_o = 2f_\# \frac{P(m+1)}{m^2} \quad (64.3)$$

Television cameras sensors are manufactured to standard sizes such as 1, 2/3, 1/2, or 1/3 in. The size is defined to be twice the horizontal dimension of a rectangular image with 4:3 aspect ratio so that a 1-in. sensor has a width of 12.7 mm, a height of 9.5 mm, and a diagonal length of 15.9 mm. Lens sizes are similarly specified to allow easy matching of lenses to sensors. Because image distortion and sharpness worsen toward the edges of the field of view, it is permissible, for example, to use a 2/3-in. lens with a 1/2-in. sensor, but not the converse. A 35-mm camera lens, designed for a 24 by 36 mm image size, generally performs much better, at relatively low cost, than a corresponding C-mount lens supplied for a TV camera but a C-mount to Pentax, Cannon, or Nikon mount converter will then be required.

It is frequently necessary to relate lighting of a scene to camera sensitivity. Accurate calculations are difficult, and it is usually better to make a simple estimate and then make fine adjustments to the lighting or lens aperture. Manufacturers often specify camera sensitivities by quoting an illumination level in lux at the sensor faceplate. This may be the illumination required to achieve maximum signal output, some proportion of this maximum, or simply a “usable” signal level from the camera. The illumination of the sensor L_S in lux is related to the luminance of the object B in cd/m^2 by

$$L_S = \frac{TB\pi}{[2f_\#(m+1)]^2} \quad (64.4)$$

where losses in the lens are characterized by a transmission coefficient T . If the object is a uniform diffuse reflector (Lambertian surface) illuminated by L_o lux, then the luminance of the object is given by

$$B = L_o \frac{R}{\pi} \quad (64.5)$$

where R is the reflection coefficient of the surface. Some practical examples of radiometric calculations are given in a Dalsa application note [7].

64.2 Image Sensing

The primary functions occurring within a standard image sensor are the conversion of light photons falling onto the image plane into a corresponding spatial distribution of electric charge, the accumulation and storage of this charge at the point of generation, the transfer or readout of this charge, and the conversion of charge to a usable voltage signal. Each of these functions can be accomplished by a variety of approaches, but only the principal sensor types will be considered here. Sensors can be divided into two groups: (1) vacuum tube devices in which the charge readout is accomplished by an electron beam sweeping across the charge in a raster fashion similar to that in a television picture tube, and (2) solid-state devices based on charge-coupled devices or photodiodes. These three types of sensor will be described in the next three sections.

Television Camera Tubes

For many years, vacuum tubes [8] provided the only technology available for television applications, and they are still widely used because of the high-quality image signals they provide. Companies supplying tubes include Burle and Philips. Most modern tube cameras are based on the vidicon design whose basic components are indicated in [Figure 64.3](#). Light from the scene is imaged by a lens onto a photoconductive target formed on the inner surface of an end window in a vacuum tube. An electron gun is placed at the opposite end of the tube to the window, and it provides a source of electrons that are focused into a beam, accelerated toward the target by a positive potential on a fine mesh placed just in front of the target, and scanned across the target by an electrostatic or magnetic deflector system. The target consists of a glass faceplate on the inner surface, upon which is placed a transparent electrically conducting coating of indium tin oxide. On top of this is deposited a thin layer of photoconductive material in a pattern of tiny squares, each insulated laterally from its neighbors. The transparent coating is connected to a positive voltage through an electrical load resistor across which the signal voltage is developed. In the absence of

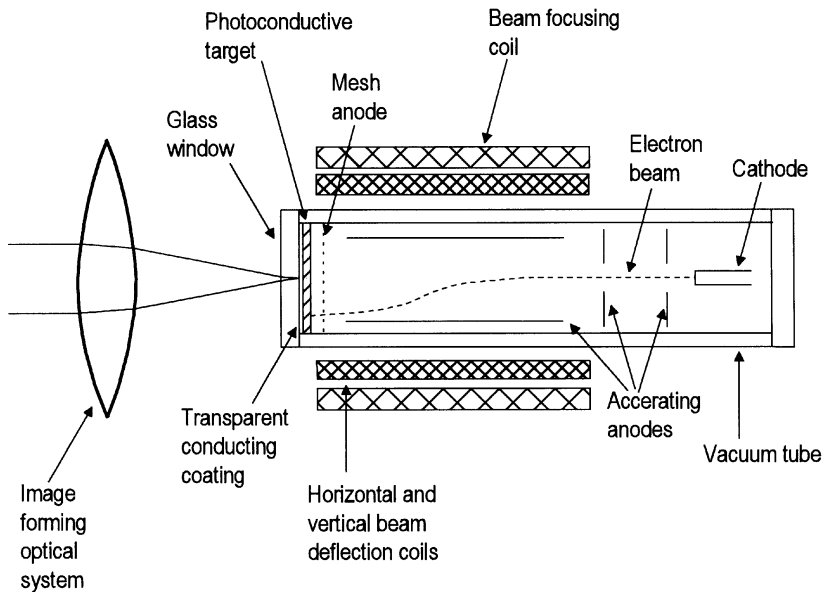


FIGURE 64.3 A schematic diagram of the major components of a vidicon camera tube. Many variants of this basic design exist utilizing different target materials to improve particular characteristics. The electron beam readout of the optically generated charge in the target makes the tube bulky and less reliable than solid-state sensors. Most tubes currently sold are for replacement in existing equipment rather than in new cameras, which almost always incorporate solid-state sensors.

light, the electron beam causes the external surface of the photoconductor to be charged to near zero potential. Light causes the resistance of the photoconductor to decrease, and its surface to acquire a more positive potential, due to the accumulation of positive charge. At each point on the surface touched by the electron beam, some of the beam current is deposited to neutralize the positive charge present due to the illumination. The rest passes through the load resistor generating an output voltage that is a function of the light intensity at that point. The precise timing of the scanning process ensures that the location of the beam is known at each instant in time.

Vidicons have some unique characteristics. They can have spectral responses extending into the ultraviolet and infrared regions of the spectrum, and they allow scan rate and adjustments in scan alignment to be made electronically by adjusting the scanning pattern. This allows very simple region-of-interest readouts. On the other hand, the electron beam readout method confers a number of disadvantages, which are not found in solid-state devices, including large size, fragility, susceptibility to shock and vibration, high power consumption and a high degree of sensitivity to external electric and magnetic fields. The principal imaging defects, which again are not present in solid-state devices, include

- lag when displaying changing images, due to slow response speed,
- image burn which is damage to the sensor surface caused by intense light,
- geometric distortion,
- drift in the apparent position of the image,
- a nonlinear relationship between signal output and light intensity which varies with target voltage.

The degree to which these effects are present depends on the type of tube and its particular construction.

The original vidicon tube design employed antimony trisulphide as the photoconductive material and a low-velocity electron beam and gave only adequate performance. Newer tubes employ the same basic design but use better electron beam readout techniques and target materials to improve characteristics such as spectral response, sensitivity, dark current, lag, and burn-in. Two tubes suitable for broadcast television use are the plumbicon developed by Philips and the saticon introduced more recently by Hitachi. The plumbicon employs a lead-oxide photoconductive target, while the saticon target comprises several layers with different combinations of selenium, arsenic, and tellurium. It can provide greater resolution than the plumbicon, but the lag performance and range of operating temperature are worse. Examples of nonbroadcast quality tubes are the newvicon, chalnicon, and the si-vidicon. The newvicon target has a double layer of cadmium and zinc tellurium, which achieves exceptional sensitivity, but lag and nonuniformity are excessive. The chalnicon employs a cadmium selenide target and provides good performance in most respects but has excessive lag. The si-vidicon target effectively consists of an array of silicon photodiodes that are reverse biased and store charge released by the incident light. The resulting tube has very high sensitivity and little lag, and it is virtually burn proof. However, it exhibits excessive blooming and nonuniformity. The silicon-intensified camera, or SIT camera, is a modification of the si-vidicon camera that employs a photocathode that generates electrons when struck by light photons. These electrons are accelerated by a voltage of several hundred volts and focused on the target of the si-vidicon sensor that produces an output in the normal way. The high-speed electrons landing on the target produce large numbers of electron-hole pairs and a corresponding larger response. The resulting SIT sensor is used in very low light level applications such as tracking satellite debris and can produce useful video images at illumination levels down to 0.001 lux. By comparison, a solid-state CCD sensor (without an image intensifier) typically requires about 1 lux to produce a useful video signal.

Charge-Coupled Devices

A CCD is fabricated on a single crystal wafer of *p*-type silicon and consists of a one- or two-dimensional array of charge storage cells on centers typically about 10 μm apart. Each cell has several closely spaced electrodes (gates) on top, separated from the silicon by an insulating layer of silicon dioxide. The charge is stored under one of the electrodes, and its location within the cell is defined by the pattern of positive voltages applied to the electrodes. By applying a coordinated sequence of clock pulses to all the electrodes

in the array, packets of stored charge (of between 10 and 10^6 electrons) are transferred from one cell to the next until they finally reach a sensing amplifier (floating gate diffusion) which generates a voltage signal proportional to charge, usually assumed to be $1 \mu\text{V}$ per electron. The result is a device that has an inherently linear variation of output voltage with light from the minimum useful level set by noise, to the maximum useful level set by saturation of the output amplifier, or the limited capacity of the charge storage cells. The dynamic range of the device is defined as the ratio of the maximum output signal to the output resulting from noise. Manufacturers published figures may use peak-to-peak or root-mean-square noise values (typically five times smaller) in this calculation, but the former is more relevant for imaging applications.

Any light penetrating into the underlying silicon generates electron-hole pairs. The holes are swept away to the substrate electrode while the electrons accumulate beneath the nearest electrode in a potential well created by the applied voltage. The sensitivity of silicon is of the order of $1 \mu\text{A}$ of generated charge per microwatt of incident light. The cells intended to function as light-sensitive photosites have electrodes made of semitransparent polysilicon so that the light can penetrate into the storage region, whereas those intended to function only as part of a shift register for charge transfer are covered by an opaque surface layer. Due to manufacturing imperfections, the photosites do not have perfectly uniform characteristics, and a photoresponse nonuniformity (PRNU) of about 5 to 10% is fairly typical. This is easy to measure using uniform sensor illumination and its effects can be removed if necessary by calibration. The basic spectral response of the silicon extends from 200 to 1100 nm, but the first figure is typically reduced to 450 nm by absorption in the surface layers of the CCD photosites. Infrared radiation penetrates deeper into the silicon than shorter wavelengths, and charge created by an infrared photon may be collected by a different cell to the one entered by the photon. This reduces the resolution of the device, and if infrared operation is not required but the illumination contains infrared (from a tungsten lamp for example), then an infrared reflecting filter (a hot-mirror filter) is often used. CCD cells also accumulate charge linearly with time due to thermally generated electrons produced within the cells and at electrode interfaces. Like the photoresponse, this dark signal varies from cell to cell and can be compensated for by calibration. These thermally generated contributions are most significant for low light level applications and can be reduced by cooling the sensor using either a thermoelectric cooler, a Joule Thomson cooler, or a liquid nitrogen dewar. The dark signal reduces by 50% for every 7°C reduction in temperature, and at -60°C , produced by a Peltier cooler, the dark signal is typically reduced to about one electron per pixel per second. Another important temperature dependent characteristic of the CCD sensor which improves with cooling is the noise floor of the output amplifier which is proportional to $T^{1/2}$ and typically equivalent to about 300 electrons at room temperature. A particular CCD device used in astronomy, for example, and operated at about -110°C has a readout noise of about 10 electrons, a dark current less than 0.3 electrons per minute, and a quantum efficiency for converting visible photons into electrons of between 70 and 80%. Light can be integrated for periods of hours, compared with the approximately 1/8 to 1/4 s integration period of the dark-adapted eye. Compared with photographic film previously used for low-light level imaging in astronomy, CCDs are from 10 to 100 times more sensitive, linear in response rather than nonlinear, and have a much greater dynamic range so that both faint and bright objects can be recorded in the same exposure.

The short-exposure, high-frequency performance of CCD devices is limited by another effect. The process of transporting charge in a CCD sensor is not 100% efficient and, in practice, a small amount of charge is left behind at each transfer to the next cell, contributing noise and degrading resolution. This effect limits the maximum clock frequency and the maximum number of transfers in a CCD sensor. Manufacturers' data sheets for commonly available CCD sensors quote values ranging from 0.9995 to 0.99999 for the charge-transfer efficiency or CTE of a single transfer. There are many variations in CCD technology. For example, virtual-phase CCDs [9] have some of the electrodes replaced by ion-implanted regions, resulting in improved blue response and higher sensitivity because of the removal of some of the blocking surface gates, and simpler drive circuitry because of the reduction in number of gates per cell. A manufacturing technique known as *pinning* can be used to passivate the interface states, which are the biggest contribution to the dark signal, producing an order of magnitude improvement in dark

signal as well as improved quantum efficiency and CTE. A signal-processing technique called *correlated double sampling* can also be applied to the output signal from the sense amplifier to improve the readout noise performance.

Linear Charge-Coupled Devices

The basic structure of a linear CCD sensor is shown in [Figure 64.4](#). It consists of a line of up to several thousand photosites and a parallel CCD shift register terminated by a sensing amplifier. Each photosite is separated from a shift register cell by a transfer gate. During operation, a voltage is applied to each photosite gate to create empty storage wells which then accumulate amounts of charge proportional to the integral of the light intensity over time. At the end of the desired integration period, the application of a transfer pulse causes the accumulated charge packets to be transferred simultaneously to the shift register cells through the transfer gates. The charges are clocked through the shift register to the sensing amplifier at a rate of up to 20 MHz, producing a sequence of voltage pulses with amplitudes proportional to the integrated light falling on the photosites. In practice, it is common for shift registers to be placed on both sides of the photosites, with alternate photosites connected by transfer gates to the right and left registers. This halves the number of cells in each register and the time required to clock out all the data. Another 2× reduction of transfer time is achieved if each shift register is split in two with an output amplifier at each end. There is a limit, typically between 10^5 to 10^6 depending on photosite size and dimensions, to the number of electrons that can be stored in a particular cell, beyond which electrons start to spill over into adjacent cells. The saturation charge in electrons is roughly 1000 to 2000 times the area of the photosite in square micrometers. This spread of charge or blooming is a problem with images containing intense highlights. It is reduced by about a factor of 100 by adding antiblooming gates between adjacent photosites and transfer gates and channel stops between adjacent photosites. The voltage on the antiblooming gates is set at a value that allows surplus charge to drain away instead of entering the transfer gates and shift register. By clocking this voltage, variable integration times that are less than the frame pulse to frame pulse exposure time can also be attained.

Area Charge-Coupled Devices

Three basic architectures are used in area CCDs and are illustrated in [Figure 64.5](#). The simplest is the full-frame CCD, consisting of an imaging area separated from a horizontal CCD shift register by a transfer

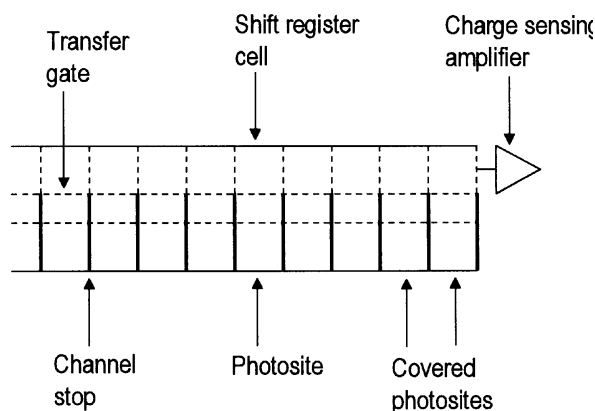


FIGURE 64.4 The architecture of a basic linear CCD showing the arrangement of photosites, transfer gates, shift register cells, and sensing amplifier. The latter produces a sequence of voltage pulses each proportional to the charge accumulated in one of the photosites. Although these pulses are often displayed on an oscilloscope during setting up of the optics and illumination, in normal use they are digitized to 8 or 12 bits, and the resulting values are stored in memory. In practice, most CCDs have two or more covered cells at each end of a line of photosites to allow the dark current to be monitored and subtracted during signal processing. Applying uniform illumination to the CCD enables the relative response of the individual photosites to be measured and compensated for.

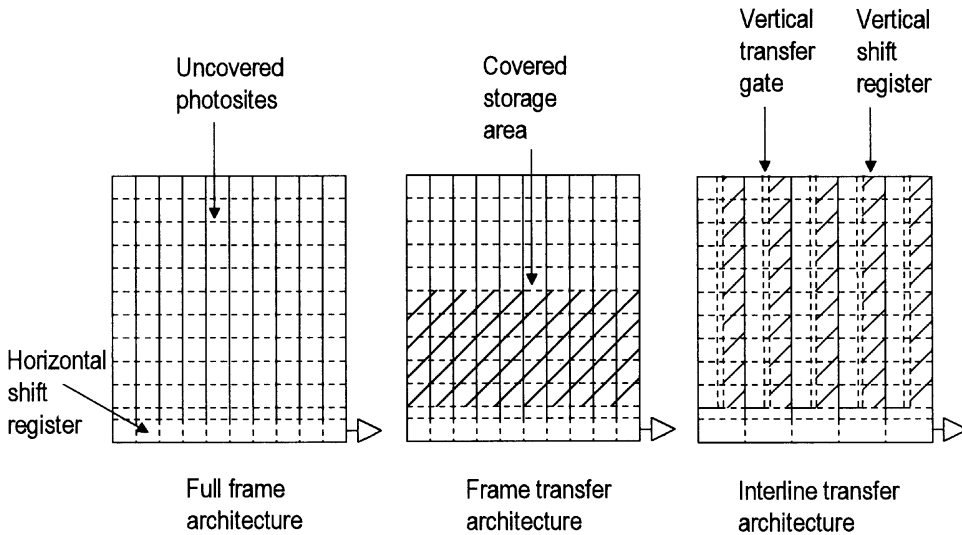


FIGURE 64.5 The basic architectures used in area CCDs. FF devices fully utilize the available area for image detection and therefore achieve the largest number of pixels, currently about 5000×5000 , but need an external shutter. FT devices are normally used at standard video rates without an external shutter. The ILT architecture allows exposure times down to less than 0.1 ms. The lower fill factor of ILT devices compared with FF and FT devices results in higher values of modulation-transfer-function at the Nyquist limit. This increases the visibility of aliasing artefacts in images containing high spatial frequencies. A low-pass optical filter must be used if aliasing is a problem.

gate. In the imaging area, each photosite is one stage of a vertical shift register separated from neighboring shift registers by channel stops and antiblooming structures. During the light integration period, the vertical clocks are stopped, creating potential wells which collect photoelectrons. At the end of this period, the charge is clocked out vertically, one row at a time, into the horizontal shift register. The charge in the horizontal shift register is then very rapidly shifted toward the output amplifier by the application of a horizontal clock signal. An example full-frame CCD is the RA1001J from EG&G Reticon, which has pixels arranged in a 1024×1024 configuration and dual horizontal shift registers and outputs to achieve a 30 frame per second readout rate. To avoid image smearing during the readout period, full-frame CCD sensors must be operated with external shutters, as in digital cameras produced by Kodak and other companies, or used in low light level applications requiring very long integration times compared with the readout time, as in astronomy. The full-frame CCD is also the basis for time delay and integration (TDI) sensor manufactured by companies such as Dalsa and EG&G Reticon. In the application of this device, which may have 96 rows each with 1024 pixels, a moving scene illuminates a region on the sensor only one pixel high, and this is arranged to move vertically down the sensor at the same rate that the generated photocharge is shifted down the sensor. This mode of operation achieves an output signal identical to that from a linear CCD sensor except for a increased light sensitivity proportional to the number of horizontal rows in the TDI sensor. It can be appropriate in applications where both high speed and high sensitivity are required, providing a cheaper alternative to the combination of a line sensor and an image intensifier. An application of this technique to capturing images of web systems moving at up to 5 m/s is described in Reference 10.

The requirement for an external shutter is greatly reduced in the frame-transfer CCD sensor by the provision of a light-shielded storage section into which the entire two-dimensional image charge is shifted at a much higher rate (limited primarily by CTE considerations) than is possible in a full-frame CCD. The charge can then be read from the storage region during the next integration period without any further image smearing. Some sensors, such as the EG&G Reticon RA1102 device, have the storage area divided into halves placed on opposite sides of the imaging area. This improves performance by halving the maximum number of transfers required to reach the nearest storage region. The same reduction

occurs automatically in sensors designed for interlaced video applications where each integration period corresponds to one video field, and only half the number of rows in the frame is required at any one time. For example, to produce an interlaced video frame containing 576 image lines (CCIR standard), a frame transfer sensor with only 288 rows of storage is required. By changing the clock signals, the odd field can be displaced vertically by half a line width relative to the even field. This ensures that the odd and even lines contain different information and reduces aliasing, because the cell width is twice the separation between the lines in the frame. Some of the companies that produce frame-transfer CCD sensors and cameras include Cohu, Dalsa, EG&G Reticon, EEV, Kodak, Philips, and Thomson-CSF.

Image smear is virtually eliminated by the interline-transfer (ILT) architecture in which each column of photosites has an adjacent light-shielded vertical CCD shift register into which the charge is transferred by a transfer pulse. The contents of all the vertical shift registers are then shifted simultaneously one pixel at a time into a horizontal shift register where they are then rapidly shifted to an output amplifier. This approach makes it easy to implement exposure control and achieve short integration times, but it introduces *dead space* between the active pixels, reducing the sensitivity of the image sensing area and increasing aliasing effects compared with frame-transfer sensors. For the latter, the fill factor, which is the percentage of the imaging area which is light sensitive, can be close to 100%, whereas it is usually less than 50% for interline-transfer devices. Localized bright objects tend to produce vertical streaks in an ILT device because strong light can leak under the narrow light shield covering the vertical shift registers, causing image smearing similar to that in a full-frame device. This reduces the usefulness of ILT sensors for scenes containing pronounced highlights. For interlaced operation, two adjacent pixels, for example 1 and 2, 3 and 4, etc., are transferred to a single shift register cell on one field, and in the next field pixels 2 and 3, 4 and 5, etc., are transferred together. This is rather similar to the interlaced operation of a frame transfer CCD. The primary advantages of the ILT sensor are low noise and good exposure control, providing true *stop-motion* control on every field, because all photosites integrate light over the same period of time. Many companies manufacture ILT CCD sensors and cameras, including Hitachi, NEC, Panasonic, Pulnix, and Sony.

The frame transfer and interline transfer approaches both have performance advantages and disadvantages, and the hybrid frame-interline transfer (FIT) approach [11] combines some of the advantages of both. This architecture includes a light-shielded field storage area between an interline imaging area and the horizontal output shift register. With this arrangement, the charge associated with the whole image is first transferred horizontally into the interline storage area, which facilitates exposure control. The charge is then transferred at maximum speed (as in the FT sensor) into the field storage area, which minimizes the occurrence of vertical streaking. For example, the NEC microPD 3541 array clocks the vertical registers at 100 times the normal rate for an ILT sensor. This gives a 20-dB improvement in streaking threshold and an overall threshold of 80 dB, making streaking effects less than other optical effects such as lens flare. On the other hand, the FIT approach does not improve the fill factor, and aliasing artefacts associated with ILT sensors and the noise levels are somewhat higher, and the CTE reduced, because of the higher clock frequencies. Manufacturers of FIT sensors and cameras include JVC, Panasonic, and Sony.

Photodiode Arrays

Because photodiode arrays generally have less extensive electrode structures over each sensing element compared with CCD arrays, the spectral response is smoother and extends further at the blue end of the spectrum. The peak quantum efficiency is also higher ranging from 60 to 80% compared with 10 to 60% for photogates, leading to almost twice the electric output power for a given light input power. Photodiode arrays would therefore appear to be attractive alternatives to CCD array sensors but, in practice, CCD sensors have lower noise levels because they do not have reverse-bias leakage current. A photodiode consists of a thin surface region of P-type silicon formed in an N-type silicon substrate. A negative voltage applied to a surface electrode reverse-biases the P-N junction and creates a depletion region in the N-silicon containing only immobile positive charge. When the electrode is isolated, the P-N junction is left

charged and is effectively a charged capacitor. Light penetrating into the depletion region creates electron-hole pairs which, with dark current, discharge the capacitor linearly with time. The penetration depth in silicon increases with wavelength and the depletion region should be wide enough to absorb all wavelengths of interest. Dark current and most of the noise sources operating in the photodiode increase with reverse bias but can be reduced by employing a thicker P-type region which allows a wide depletion region to be achieved with low bias voltage. However, this also degrades the blue-end response of the photodiode. To achieve good blue and UV response along with low bias voltage operation, a three-layer structure comprising thin P-type, intrinsic, and N-type substrates is employed. The intrinsic layer is so pure that the depletion region extends halfway across it at zero bias and extends right across it at a small reverse bias voltage. This structure provides photodiodes with excellent linearity, noise performance, and speed of response at low operating voltages. At the end of an integration period, the states of charge of the photodiodes are measured, and image sensors based on two different types of readout approach are commercially available. These are the serially switched (sometimes called self-scanned) photodiode (SSPD) arrays and the charge-coupled photodiode (CCPD) arrays illustrated in [Figure 64.6](#).

Serially-Switched Photodiode Arrays

Associated with each photodiode in the sensor array is an MOS (metal-oxide semiconductor) switch which, when turned on by a digital voltage level applied to its control line, connects the photodiode to a readout amplifier. Each control line is connected to one of the outputs of a digital shift register and, shifting a bit through the register, sequentially reads the charge on each photodiode in the array. This type of readout is very flexible, and random readout is achieved by replacing the digital shift register by an address decoder connected to an address bus as in the SR series linear arrays from EG&G Reticon. 2-D arrays of photodiodes are connected in a configuration similar to a cross-point switching matrix with a switch and diode at each cross point and separate vertical and horizontal shift registers. To scan the array, the vertical shift register turns on a complete row of switches, which causes the photodiodes in the corresponding row to dump their charge into vertical signal lines. These are in turn connected to the output amplifier by a set of horizontal switches controlled by the horizontal shift register. Switched arrays of photodiodes are made using processes similar to those employed in the manufacture of dynamic RAM, and this along with their simple structure and small size, yields higher densities and lower manufacturing costs. However, the SSPD approach has one shortcoming, namely the large capacitances of the readout buses. This reduces the speed of the device, increases the noise, and reduces the dynamic range, which are all generally significantly worse than those of CCD sensors. The dynamic range for

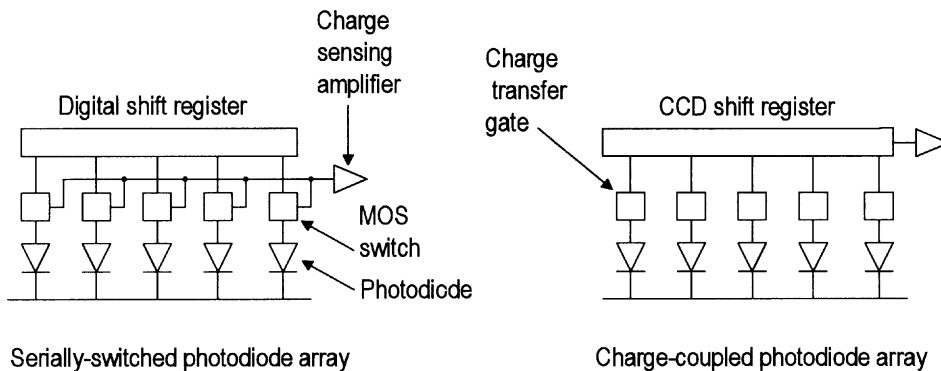


FIGURE 64.6 Readout architectures associated with photodiode array sensors. In the SSPD approach shown, each photodiode is connected in turn via an MOS switch to the sensing amplifier. This eliminates smearing, because the charge does not move between photosites. The device noise and speed characteristics are poorer than CCD sensors because of nonuniformity in the MOS switches and the large capacitance of the sensing bus. The CCPD approach combines the excellent blue end response of the photodiode with the low noise transfer characteristics of the CCD shift register to produce very high-quality linear devices.

example is typically 250 to 300 compared to more than 2500 for commercially available CCD sensors. SSPD arrays also suffer from fixed-pattern noise due to nonuniformities in the switches, which can be as high as 20% of the saturated output. The SSPD approach does have unique advantages:

- The readout method is extremely flexible and can be programmable.
- It is relatively free from blooming effects, because the sensors can be optimally isolated from each other.
- The blue response is good, which is particularly important for spectroscopic applications and for studio quality color television cameras.

Manufacturers supplying SSPD-based sensors include EG&G Reticon, Hamamatsu and VLSI Vision.

Charge-Coupled Photodiode Arrays

Although individual photodiode elements are superior to individual CCD photogate elements in terms of dynamic range, the dynamic range of the SSPD is limited by fixed pattern noise, switching noise and the difficulty of transferring charge packets over the high capacitance output bus. Replacing the horizontal digital shift registers by a low noise CCD shift register significantly improves the dynamic range of the device and the resulting hybrid design is the charge-coupled photodiode array. During operation, the charges on an entire row of photodiodes are simultaneously transferred via MOS switches into the analog CCD shift register and then shifted out in sequence to the output amplifier. By providing a reset pulse (from a second vertical digital shift register) to eliminate all pre-stored charge in one row a fixed interval before the charge is transferred to the CCD shift register, it is relatively easy to implement an electronic equivalent of a focal plane shutter [12] and control exposures in increments of one horizontal scan period. However, images of moving objects will be subject to distortions similar to those found using photographic cameras with focal-plane shutters. In the case of 2-D arrays there are inefficiencies in the movement of small charge packets over the vertical transport lines which get worse the smaller the packet. The solution adopted is to turn a small charge into a large one by pre-charging the lines with a priming charge equal to 10 to 15% of the maximum charge capacity before transferring the photo-charge to the CCD in a process known as charge-primed transfer. This requires several MOS switches forming a sequence of transfer gates and storage capacitors between each vertical transport line and CCD cell and depends critically on correct phasing of a large number of timing signals for proper operation. The CCPD approach appears to be most successful for linear arrays which do not require a vertical transport bus. Manufacturers supplying linear CCPD based sensors include Dalsa and EG&G Reticon.

64.3 Image Intensifiers

When the available solid-state image sensors do not have enough sensitivity for the scene illumination, it is necessary either to use a more sensitive tube camera or to amplify the available light. Companies supplying intensified cameras include Cohu, Kodak, Pulnix, and Philips. Intensified cameras are standard video cameras fitted with image intensifiers that increase the number of available photons falling onto the image sensor. In addition to allowing operation over a wide range of lighting of the order of 0.0001 lux from overcast starlight to 100,000 lux of full sunlight, intensified cameras can be used to stop motion in nanosecond frame times, count photons, and observe images with very high intrascene dynamic ranges. However, this increased flexibility is achieved at a considerable increase in cost, usually some loss in resolution, reduced lifetime, and increases in geometrical distortion, lag, and smear. Image intensifier tubes (IITs) are usually classified as generation I, II, and III devices.

Generation I Tubes

In a generation I intensifiers, illustrated in [Figure 64.7](#), the incoming photons strike a multi-alkali photocathode within a vacuum tube, and the resulting photoelectrons emitted into the vacuum are accelerated and focused onto a phosphor coating on the rear wall of the tube. The impact of the high-energy

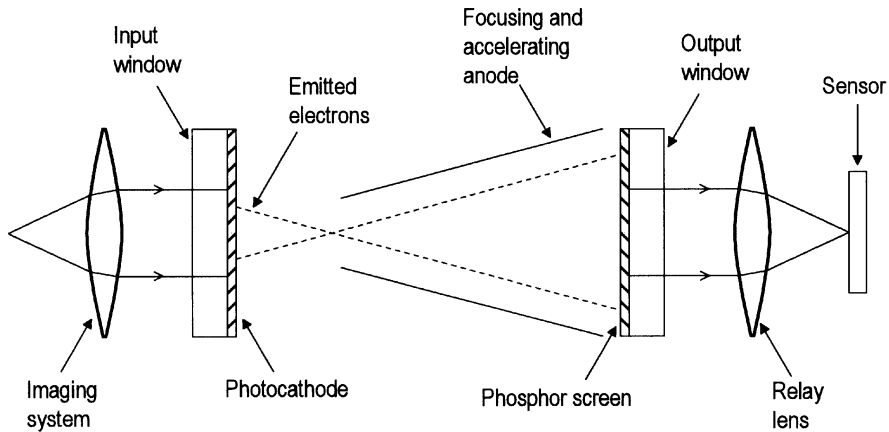


FIGURE 64.7 A schematic diagram showing the major components of a generation I image intensifier tube coupled to a sensor. Combined with a CCD sensor, the sensitivity of a SIT tube camera is achieved but with much higher reliability and greatly reduced lag, geometrical distortion, and power consumption. An example is the Cohu 5512 generation I optical-fiber coupled intensified CCD camera, sensitive down to 0.00015 lux and with 460 TV lines horizontal resolution, currently costing about \$12,000.

electrons on the phosphor creates many electron-hole pairs that in turn generate light at a higher level than that striking the photocathode. The electron gain depends strongly on the accelerating voltage and also on the photocathode and phosphor materials, and it is typically around 200 with a 12 kV accelerating voltage. These tubes tend to be bulkier than later-generation tubes and have relatively low gains, although tubes can be cascaded to achieve higher gains. They are also relatively intolerant of bright sources and rapid changes of scene illumination, with increased tendency toward highlight blooming. The light output from the intensifier tube is transferred to the solid-state sensor by either a relay lens or a fiber-optic coupler. The latter is shorter and much more efficient (typically 60% compared with 6%), but requires a sensor whose protective glass or quartz window has been replaced by the fiber-optic coupler resting against the sensor surface. The narrow gaps between couplers and between the coupler and sensor are filled by an index-matching optical grease. The spectral response of the photocathode should be chosen to match the scene requirements, while the narrower phosphor response should be optimally matched to the image sensor for greatest sensitivity [13]. In general, for largest output, a phosphor with the maximum persistence that is acceptable in terms of image lag should be selected. But, if the scene includes object motion, a shorter-persistence phosphor may be necessary to avoid image smear. For night vision, P20 and P39 phosphors are frequently used. The former emits 550 nm light with very high luminous efficiency (65%) and relatively short persistence (0.2 ms), while the latter has a persistence of about 80 ms, which reduces high-frequency jitters. For high-speed imaging, the yellowish-green P46 phosphor has a persistence of only 0.16 μ s, while the purplish-blue P47 phosphor has a persistence of only 0.08 μ s. However, both these phosphors have luminous efficiencies of only 3%. The resolution of an intensified camera is generally quoted in line pairs per millimeter (lp/mm) and is the harmonic mean of the individual resolutions of the intensifier (typically 20 to 30 lp/mm), the coupler (typically 80 lp/mm), and the image sensor (typically 20 to 50 lp/mm).

Generation II and III Tubes

Generation II intensifiers are similar to generation I devices except that gain is achieved using a micro-channel plate (MCP) instead of an accelerating potential difference in vacuum (see Fig. 64.8). Generation III intensifiers are similar to generation II except that the multialkali photocathode is replaced by a gallium arsenic solid-state structure. The resulting device has double the gain of a type II device and improved SNR and resolution. The heart of both types is an MCP disk about 25 mm dia. and 0.5 mm thick, consisting of an array of millions of glass tubes (called *microchannels*) with holes about 10 μ m diameter

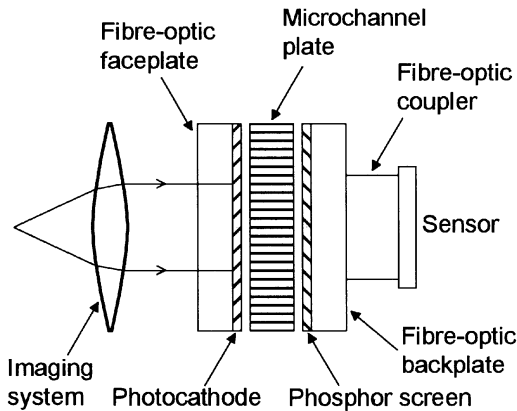


FIGURE 64.8 The basic components of a generation II or III intensified-image sensor. These are typically two and four times more sensitive than generation I intensifiers. Narrow vacuum gaps between the photocathode, microchannel plate, and phosphor screen achieve proximity focusing. An example is the Philips I800 low-light video camera, which couples an XX1410 generation image intensifier with an FT800 1/2-in., 760×576 resolution frame-transfer CCD at a cost of around \$8000.

coated with a secondary electron emitting substance. The two faces of the MCP are coated with conducting layers, allowing a voltage (typically 50 to 900 V) to be applied between the entrance and exit of each microchannel. An energetic electron from the photocathode enters a microchannel and produces secondary electrons on striking the wall. These electrons are accelerated by the axial electric field and, in turn, dislodge more secondary electrons. This process is repeated many times down the channel. The number of electrons continues to increase until either the end of the channel is reached or current saturation occurs because the electron cloud is so dense that it inhibits further secondary emission. The electrons exit the MCP and may be accelerated further before striking a phosphor screen. The light generated is then transported to the image sensor by fiber-optic couplers. A thick phosphor layer increases light gain but allows electrons and light scattering in the phosphor, which causes some loss of resolution. Improved performance is achieved by integrating the phosphor into the fiber-optic bundle in a so-called *intagliated construction*. Each glass core in the fiber-optic bundle is etched out to a predetermined depth, leaving a small cup of cladding glass at the entrance to each fiber, which is filled with phosphor. Electrons striking the phosphor produce light that is confined to one fiber, minimizing crosstalk and improving resolution. The overall light amplification achieved is of the order of 10^4 , and higher gains can be achieved by stacking multiple MCPs and by increasing the accelerating voltages. The MCP has a nonlinear response, because the current density increases at an exponential rate until limited by saturation. The IIT can be gated in only a few nanoseconds by pulsing the cathode potential from the cutoff level (a few volts positive) to the normal operating voltage. This provides a high-speed shutter capability for stopping motion as well as a means of exposure control. Generation II devices have high gain and dynamic range and are easy to gate on and off, but they have relatively low output levels compared with generation I devices. The Kodak EktaPro 1000 high-speed video camera uses a generation II intensifier as a high-gain first stage coupled to a generation I intensifier to provide the required level of light output.

64.4 Fiber Optic Scopes

It is sometimes necessary to acquire images within confined and inaccessible spaces. In some cases, this can be achieved with the aid of mirrors, but when the image must be conducted around bends, a fiberscope may be needed. This consists of a semirigid flexible sheathing around a bundle of optical fibers, each about $10 \mu\text{m}$ diameter aligned coherently so that fibers have the same relative location at entrance and exit of the bundle. An image formed on one end of the bundle therefore appears undistorted but dimmer

at the other end. Between 20 and 35% of the bundle face area consists of fiber cladding and epoxy filler and does not transmit light. Light passing through fiber cores suffers Fresnel reflection losses of about 4% on entering and leaving, and attenuation within the fibers of the order of 10 to 15% for each meter of length. A 1 m fiberscope therefore transmits only about 40 to 60% of the incident light. Fiberscopes range in diameter from about 2 to 18 mm and in length from about 0.6 to 3 m, with a minimum bend radius of about 75 mm for an 8 mm insertion diameter tube. To illuminate the object, a coaxial arrangement of fibers is often used, as in the flexible boroscope marketed by Edmund Scientific. The inner fibers are used for imaging, while fibers in the outer, noncoherent bundle are used to transport light to the object. Alternatively, a separate fiber-optic light guide may be used. Fiberscopes may be fitted with optics for viewing in the forward, oblique, side, and rearward directions but may not allow easy quantitative measurements of distances and areas because of distortions introduced by wide-angle optics. Fiberscopes are generally supplied with an eyepiece for direct observation, but C-mount couplers are often available to allow a CCD camera to be connected.

64.5 Components and Trends

A wide range of image sensors and cameras based on tube and solid-state technologies is now available, and a few examples are listed in [Table 64.1](#) to give an indication of some of the currently available devices and their approximate prices, if purchased in the U.K. It is advisable to contact local suppliers to determine actual prices and availability. Contact information for some companies is listed in [Table 64.2](#). Manufacturers are continuing the incremental development of sensors with greater resolutions, readout rates, and signal-to-noise performances, and new application areas such as high-definition television (HDTV) and digital photography should cause prices to come down as the markets for these products expand. Some examples of this type of development are as follows.

- EG&G Reticon is currently developing a 1000 frames per second, 1024×1024 interline-transfer CCD sensor for high-speed imaging.
- Thomson Components (France) has developed the THX-31163 CCD sensor specifically for use in HDTV. This chip is designed to output 1152×1260 pixel frames in 40 ms at a transfer frequency of 47 MHz.
- Manufacturers such as Kanimage, Kodak, and Leaf Systems supply digital cameras based on very high-resolution area array sensors. The Kodak professional range of color and monochrome digital cameras, for example, incorporate CCD full-frame transfer sensors with resolutions ranging from 1024×1536 to 2036×3060 into standard 35 mm photographic cameras.

A separate trend is the development of smart cameras and smart sensors [14] for industrial and scientific applications. There are two basic motivations. One is to correct for imperfect behavior of sensors (such as pixel to pixel nonuniformity associated with MOS devices), and the other is to reduce the communications or processing bottlenecks associated with handling very large amounts of image data. A smart camera is a single-image acquisition subsystem incorporating image sensor, analog-to-digital conversion, and microprocessor that provides processed image data in a standard format such as SCSI or RS-423. Pulnix already supply a series of smart linescan cameras that implement application functions such as object detection, size measurement, and go, no-go comparison. Another example is the imputer 3 [15] from VLSI Vision incorporating a CMOS (complementary MOS) area sensor with 512×512 digital resolution and an i960 32-bit reduced instruction set processor. Using VLSI technology, but not CCD technology, it is possible to integrate both image acquisition and low-level processing onto a single chip to achieve a kind of electronic retina. One way of constructing such chips is to integrate photodetector and processing element at the photosite, but this produces very poor fill factors. This can be alleviated to some extent by using microlenses to focus the light onto the sensitive region. An alternative approach is to implement the photodetection and processing as separate arrays on the chip. This allows a large fill

TABLE 64.1 Cameras, Sensors, and Other Components

Manufacturer	Designation	Function	Specification	Approximate price
Cohu	4712	Monochrome TV camera	1/2-in. FT CCD, 754 × 484 pixels, 0.04 lux minimum, RS-170 output	\$2,000
Cohu	4110	Digital output camera	1/2-in. FT CCD, 755 × 484 pixels, 0.01 lux minimum, 8-bit per pixel RS-422 outputs	\$4,000
Cohu	4912	Monochrome TV camera	1/2-in. ILT CCD, 768 × 494 pixels, 0.02 lux minimum, RS-170 output	\$1,000
Cohu	2252	Color TV camera	1/2-in. microlens ILT CCD, CMYG mosaic filter, 0.3 lux minimum, NTSC/Y-C/RGB outputs	\$1,400
Edmund Scientific	A52999	Fiberscope	8 mm diameter, bend radius 75 mm, 60° field, 10 to 100 mm focus	\$1,200
EG&G Reticon	D Series	Line sensors	256, 512, 1024, or 2048 pixel CCPD arrays	\$80 to \$2,400
EG&G Reticon	LC1911	Line scan camera	10 MHz data rate, D series sensors, RS-422 outputs	\$2400
EG&G Reticon	RA1001	Area sensor	FF CCD, 1024 × 1024 pixels, dual outputs, 30 frames per second	\$2,500 to \$16,000, depending on grade
EG&G Reticon	TD Series	TDI CCD array	1024 × 96 pixels, single output	\$400
Hamamatsu	S5464-1024Q	Spectroscopic line sensor	CMOS SSPD 1024 array, 2.5 mm by 25 μm pixels, quartz window	\$1,600
Kodak	DCS 410	Color digital camera	FF CCD, 1524 × 1012 pixels, mosaic filter, Nikon N90S camera	\$8,800
Kodak	DCS 460	Color digital camera	FF CCD, 3060 × 2036 pixels, mosaic filter, Nikon N90S camera	\$4,0000
Panasonic	GP-US502	Remote head color camera	3 1/2-in. ILT CCDs, 768 × 494 pixels, 3 lux minimum, NTSC/Y-C/RGB outputs	\$7,500
Philips	XX1410	Intensifier	18 mm generation II	\$1,600
Philips	XQ3427	Tube	2/3-in. plumbicon, 400 TV lines at 55% modulation	\$3,200
Philips	XQ1270	Tube	2/3-in. vidicon, resolution 500 TV lines	\$120
VLSI Vision	Imputer 3	Intelligent camera	2/3-in. CMOS sensor, 512 × 512 × 8-bit, 32-bit RISC CPU	\$4,000
VLSI Vision	IDS	Development system	Software and hardware to create Imputer 3 applications	\$7,200

TABLE 64.2 Some Manufacturers of Image Sensors and Cameras

Burle Industries Inc., Tube Products Division 1000 New Holland Avenue Lancaster, PA 17601-5688 Tel: (800) 366-2875 Fax: (717) 295-6096	Cohu Inc., Electronics Division 5755 Kearny Villa Rd. San Diego, CA 92123 Tel: (619) 277-6700 Fax: (619) 277-0221
Dalsa Inc. 605 McMurray Road Waterloo, Ontario, Canada N2V 2E9 Tel: (519) 886-6000 Fax: (519) 886-8023	Eastman Kodak Company 343 State Street Rochester, NY 14650 Tel: (800) 235-6325 Internet: http://www.kodak.com
Edmunds Scientific Company, International Dept. Meg DiMinno Barrington, NJ 08007 Tel: (609) 573-6263 Fax: (609) 573-6882	EEV Ltd. Waterhouse Lane Chelmsford, Essex CM12QU, U.K. Tel: 01245 453652 Fax: 01245 492492
EG&G Reticon, Western Regional Sales 345 Potrero Avenue Sunnyvale, CA 94086 4197 Tel: (408) 738-4266 Fax: (408) 738-6979	Hamamatsu Photonix (U.K.) Ltd. 2 Gladbeck Way Windmill Hill, Enfield, Middx. EN2 7JA Tel: 0181 367 3560 Fax: 0181 367 6384
Hitachi Denshi (U.K.) Ltd. 14 Garrick Ind. Ctr. Irving Way, Hendon London NW9 6AQ Tel: 0181 2024311 Fax: 0181 2022451	NEC Electronics (U.K.) Ltd. Sunrise Parkway Linford Wd, Milton Keynes, Bucks. MK14 6NP Tel: 01908 691133 Fax: 01908 670290
Panasonic Industrial Europe U.K. Willoughby Road Bracknell, Berks RG12 4FP Tel: 01344 853087 Fax: 01344 853706	Philips Components Ltd. Mullard House Torrington Place London WC1E 7HD Tel: 071 5806633 Fax: 071 4362196
Pulnix America Inc. 1330 Orleans Drive Sunnyvale, CA 94089 Tel: (408) 747-0300 Fax: (408) 747-0660	Sony Broadcast & Professional Europe Image Sensing Products Schipolweg 275 1171 PK Badhoevedorp Amsterdam, The Netherlands Tel: 020 658 1171 Tel: (U.K.) 01932 816300
Thomson-CSF Unit 4, Cartel Business Centre Stroudley Road Basingstoke, Hants RG4 0UG, U.K. Tel: 01256 843323 Fax: 01256 23172	VLSI Vision Ltd., Aviation House 31 Pinkhill Edinburgh EH12 7BF, U.K. Tel: 0131 5397111 Fax: 0131 5397141

factor but requires high-frequency data paths between the two arrays. The development of smart image sensors is still in its infancy, but nevertheless the creation of an artificial eye is now on the horizon.

References

1. T. N. Cornsweet, *Visual Perception*, New York: Academic Press, 1970.
2. CCIR, *Characteristics of Monochrome and Colour Television Systems*, Recommendations and Reports of the CCIR, Vol. XI, Part 1: Broadcasting Service (Television), Section IIA, 1982.

3. W. Booth, S. S. Ipson and Y. Li, The application of machine vision and image simulation to the fabrication of knives used for cutting leather, *Proceedings of ACCV'95, Second Asian Conference on Computer Vision*, 5–8 December 1995, Singapore, II574–II578.
4. R. K. Hopwood, Design considerations for a solid-state image sensing system, Reprint from *Proceedings of SPIE*, 230, 72–82, 1980 In *EG&G Reticon 1995/6 Image Sensing and Solid State Products*.
5. S. F. Ray, *Applied Photographic Optics*, 2nd. ed., Oxford, U.K.: Focal Press, 1994
6. Depth of field characteristics using Reticon's image sensing arrays and cameras, Application note 127 In *EG&G Reticon 1995/6 Image Sensing and Solid State Products*.
7. Practical radiometry, Application note in *Dalsa CCD Image Capture Technology, 1996–1997 Databook*.
8. S. J. Lent, Pickup tubes and solid-state cameras, in K. G. Jackson and G. B. Townsend (eds.), *TV & Video Engineers Reference Book*, Oxford, U.K.: Butterworth-Heinemann, 1991.
9. L. Sheu and N. Kadekodi, Linear CCDs, Advances in linear solid-state sensors, *Electronic Imaging*, August 1984, 72–78.
10. S. C. Chamberlain and P. T. Jenkins, Capturing images at 1000 feet per minute with TDI, *Photonics Spectra*, 24(1), 155–160, 1990.
11. D. A. Rutherford, A new generation of cameras tackles tomorrow's challenges, *Photonics Spectra*, 23(9), 119–122, 1989.
12. A. Asano, MOS sensors continue to improve their image, *Advanced Imaging*, 42–44f, 1989.
13. C. L. Rintz, Designing with image tubes, *Photonics Spectra*, 23(12), 141–143, 1989.
14. J. E. Brignell, Smart sensors, in *W. Gopel, J. Hesse and J. N. Zemel (eds.), Sensors: A Comprehensive Review, Volume I: Fundamentals*, Weinheim, WCH Publications, 1989
15. O. Vellacott, VLSI Vision Review note, CMOS in camera, *IEE Review*, 40(3), 111–114, 1994.

Further Information

M. W. Burke, *Image Acquisition: Handbook of Machine Vision Engineering, Vol. I*, London: Chapman and Hall, 1996. Provides comprehensive coverage of lighting, imaging optics and image sensors.

Dalsa CCD Image Capture Technology, 1996–1997. Databook includes useful application notes and technical papers on image sensors and TDI.